Coherent and diffusive fields of underwater acoustic ambient noise

V. A. Shchurov
Pacific Oceanological Institute, Far Eastern Branch of USSR Academy of Sciences, Vladivostok, USSR

(Received 2 March 1990; accepted for publication 16 January 1991)

In this paper, results of investigations of underwater ambient noise are presented based on statistical analysis of the acoustic pressure and three orthogonal components of particle velocity of a medium $P(t)$, $V_x(t)$, $V_y(t)$, $V_z(t)$. The mathematical analysis used includes cross-spectral characteristics, simple coherence functions, phase spectra, and an algorithm to split the noise field into anisotropic and isotropic fields. The above approach is applied to study the anisotropic and isotropic fields of ambient noise in the deep open ocean and in a coastal area. A fundamental feature of the anisotropic field that has been revealed is that the direction of the horizontal component of dynamic noise energy flux is similar to the surface roughness propagation direction.

PACS numbers: 43.30.Nb

INTRODUCTION

Here we understand the vector-phase measurements in a nonmoving medium as a simultaneous measurement of the acoustic pressure field $P(t)$ and three orthogonal components of the particle velocity vector of the medium $\mathbf{V}\{V_x(t), V_y(t), V_z(t)\}$ made at a given point. Totality of the vector-phase measurements and of the corresponding mathematical methods allowing calculation of the Umov–Pointing vector of the energy flux density and its characteristics will be considered as a vector-phase technique in acoustics.

A device that simultaneously measures P, V_x, V_y, and V_z, and that consists of a pressure receiver and a three-component receiver, will be further referred to as a combined receiver in our paper.[1]

The first instrument to measure the air flow sound energy density vector was described by H. D. Olsen in 1932. The first modern-type receiver of the particle velocity based on an electrodynamic transducer constructed by "Bell Telephone Laboratories" for the U.S. Naval Laboratory of hydroacoustic measurements appeared in 1942.

At present various techniques have been developed for measuring the acoustic field energy flux vector in nonmoving media in both aero- and hydroacoustics.[2–13] Analog and digital procedures have also been worked out to process the acoustic data.[8,14–20] According to incomplete information, from the middle of the 1940's to the middle of the 1970's in Great Britain, USSR, USA, France, and Japan there were registered more than 140 patents on the principles of constructing the particle velocity receivers (pressure gradient receivers) and application of those measuring systems to solve problems in aero- and hydroacoustics. However, there are few works published dealing with investigations of the vector-phase characteristics of the acoustic fields in the ocean. In the present paper, an attempt has been made to show some results of the many-year studies on underwater acoustic ambient noise using the vector-phase technique. Anisotropic and isotropic properties of the underwater ambient noise field are discussed based on consideration of the interrelation between the acoustic pressure and particle velocity in this field. Also, this paper uses the results of works published in Russian in 1981–1990.[1,14,21–28]

In Sec. I of this paper, theoretical and technical aspects of the vector-phase technique are presented. In Sec. II the results of investigations are discussed.

I. THEORETICAL AND TECHNICAL ASPECTS OF THE VECTOR-PHASE TECHNIQUE

A. Basic physical relationships

Following Refs. 29–32, we present basic theoretical relationships for the energy characteristics of the acoustic field.

The instantaneous value of energy density of the acoustic field of a plane traveling harmonic wave is

$$E(t) = E_{\text{kin}}(t) + E_{\text{pot}}(t) = \frac{1}{2}\rho V^2(t) + \frac{1}{2}\frac{P^2(t)}{\rho C^2} = \frac{P^2(t)}{\rho C^2}, \tag{1}$$

since $E_{\text{kin}}(t) = E_{\text{pot}}(t)$.

In Eq. (1), the following notation is introduced: $P(t)$ and $V(t)$ are instantaneous values of the acoustic pressure and particle velocity, respectively; C is a sound velocity; ρ is an equilibrium value of the density of a medium; and $E_{\text{kin}}(t)$ and $E_{\text{pot}}(t)$ are instantaneous values of kinetic and potential energy densities, respectively.

The mean density of total energy averaged "temporally" or "spatially" is equal to the maximum amplitude value of the kinetic (potential) energy density,

$$\langle E(t)\rangle = \frac{1}{2}\rho V_0^2 = \frac{1}{2}\frac{P_0^2}{\rho C^2}, \tag{2}$$

where P_0 and V_0 are the amplitude values of the pressure and particle velocity, respectively.

In accordance with a virial theorem,[32] the ratio for the mean values in Eq. (2) in the acoustic wave is also true for arbitrary variations in a small amplitude.

The acoustic energy change in some volume v limited to the closed surface s can be written as[31,32]

$$\frac{\partial}{\partial t}\int_v E(t)dv = -\oint_s P(t)\mathbf{V}(t)d\mathbf{s}. \quad (3)$$

The right-hand expression beneath the integral is the instantaneous value of the energy flux density vector $\mathbf{I}(t)$ (Umov–Pointing vector)

$$\mathbf{I}(t) = P(t)\mathbf{V}(t), \quad (4)$$

which shows the direction of transfer and the value of the energy passing through the unit area per unit of time.

For the simplest case of a plane traveling monochromatic wave field from one source in an infinite homogeneous medium the averaged vector of the energy flux density intensity is oriented toward the direction of the wave movement $\mathbf{n}$ and can be represented by the following expression:

$$\mathbf{I} = \langle \mathbf{I}(t) \rangle = \frac{1}{2} P_0 V_0 \mathbf{n} = \frac{1}{2}\rho C V_0^2 \mathbf{n} = \frac{1}{2}\frac{P_0^2 \mathbf{n}}{\rho C}, \quad (5)$$

where P_0 and V_0 are amplitude values of the pressure and particle velocity, respectively.

If the acoustic field at some point in space is represented by a superposition of plane waves arriving from the various directions there, then the magnitude of the resulting averaged energy flux I_r along some direction $\mathbf{r}$ may be written as a sum of separate flows projectioned on the given direction:[30]

$$I_r = \frac{1}{2}\sum_{i=1}^{n} P_{0i} V_{0i} \cos\psi_i, \quad (6)$$

where P_{0i} and V_{0i} are i-wave amplitude values of the pressure and particle velocity, respectively; ψ_i is an angle between the directions of the particle velocity vector of the i-plane wave and the r direction. The component I_r expressed through amplitudes of resulting values of the acoustic pressure p_0 and particle velocity component V_{0r}, is then

$$I_r = \tfrac{1}{2} P_0 V_{0r} \cos(\varphi_p - \varphi_v), \quad (7)$$

where $(\varphi_p - \varphi_v) = \varphi_{pVr}$ is the phase difference between the pressure and particle velocity in a resulting wave.

Equations (5)–(7) give the mean intensity of the acoustic field calculated at the time interval $t \geqslant T$ (T is a period of the monochromatic wave).

The vector-phase measurements result in the following acoustic field characteristics which are random values of time:

(i) $P(t)$, $V_x(t)$, $V_y(t)$, $V_z(t)$ are instantaneous values of the acoustic pressure and orthogonal components of the particle velocity, respectively;

(ii) $\varphi_{px}(t)$, $\varphi_{py}(t)$, $\varphi_{pz}(t)$ are instantaneous values of the phase difference between the pressure and particle velocity components, respectively;

(iii) $\varphi_{xy}(t)$, $\varphi_{xz}(t)$, $\varphi_{yz}(t)$ are instantaneous values of the phase difference between the corresponding components of the particle velocity.

We limit statistical analysis of these values in time and space to cross-correlation analysis.[29] In the time domain, the cross-correlation function of two random processes $P(t)$ and $V_r(t)$,

$$R_{pV_r}(\tau) = \langle P(t) V_r(t+\tau) \rangle, \quad (8)$$

at $\tau = 0$ is the energy flow of the acoustic field along the r direction,

$$R_{PV_r}(0) = \langle P(t) V_r(t) \rangle = I_r. \quad (9)$$

In the frequency domain, we have the following:

(i) $S_{p^2}(f), S_{V^2}(f)$ are autospectra of the pressure and particle velocity, respectively;

(ii) $S_{PV_r}(f)$ is a mutual spectrum of the pressure $P(t)$ and particle velocity component $V_r(t)$;

(iii) the simple coherence function is

$$\gamma^2_{PV_r}(f) = |S_{PV_r}(f)|^2 / S_{p^2}(f) S_{V_r^2}(f); \quad (10)$$

(iv) the phase spectrum is

$$\varphi_{PV_r}(t) = \arctan|\mathrm{Im}(PV_r^*)/\mathrm{Re}(PV_r^*)|; \quad (11)$$

where $V_r^*(t)$ indicates the complex conjugate value of $V_r(t)$ and $\mathrm{Re}(PV_r^*)$ and $\mathrm{Im}(PV_r^*)$ are active and reactive powers of the field, respectively, which are included into the mutual spectrum modulus

$$|S_{PV_r}(f)| = \sqrt{\mathrm{Re}^2(PV_r^*) + \mathrm{Im}^2(PV_r^*)}. \quad (12)$$

For the random processes $P(t)$ and $V_x(t)$, $V_y(t)$, $V_z(t)$ we have: the autospectra

$$S_{p^2}(f), S_{V^2x}(f), S_{V^2y}(f), S_{V^2z}(f);$$

the mutual spectra

$$S_{PVx}(f), S_{PVy}(f), S_{PVz}(f),$$
$$S_{VxVy}(f), S_{VxVz}(f), S_{VyVz}(f);$$

coherence functions

$$\gamma^2_{PVx}(f), \gamma^2_{PVy}(f),$$
$$\gamma^2_{PVz}(f), \gamma^2_{VxVy}(f), \gamma^2_{VxVz}(f), \gamma^2_{VyVz}(f);$$

and phase spectra

$$\varphi_{PVx}(f), \varphi_{PVy}(f), \varphi_{PVz}(f),$$
$$\varphi_{VxVy}(f), \varphi_{VxVz}(f), \varphi_{VyVz}(f).$$

A set of these functions allows us to separate the anisotropic and isotropic components of the underwater ambient noise field and to examine their properties.

B. Technique of investigations

1. Principle of measuring the particle velocity

In the investigations carried out, the combined receiver has been employed with a hull moving together with the medium. Description of the theoretical and practical aspects of the measurements by means of this receiver can be found in the literature.[1-6,13,30,32-35] Here we consider the principle of its operation. The receiver is a hard sphere with built-in transducers and is secured with flexible rubber cords in a sonar dome. The amplitude of the velocity of the hard sphere variations (V) (the sphere's mean density is ρ) in incompressible fluid (density ρ_0) in a plane sound wave (amplitude of the velocity V_0) is expressed by the relationship:

$$V = [3\rho_0/(2\rho + \rho_0)]V_0.$$

Analysis shows that, if the radius of the hard sphere a is smaller than $\lambda/6$ of an incident wave and the mean density of the sphere ρ approaches the fluid density ρ_0, then the veloc-

ity of the sphere movement approaches that of the particle's movement of a medium in the sound wave.[13,32]

2. Combined receiver and its characteristics

The receiver of the particle velocity used represents a single spheroplastic ball of diameter 0.2 m with piezoceramic transducers inserted. Three pairs of the transducers are located in pairs and symmetrically relative to the center of the sphere on the orthogonal axes x,y,z [Fig. 1(a)].

The first resonance frequency f_1 of the transducers used lies in the frequency range 1.5–2.0 kHz. In the working frequency range $f<f_1$ the electric signal from each pair of the transducers is proportional to the corresponding component of the particle's acceleration $a_x(t)$, $a_y(t)$, $a_z(t)$. The working range is limited to below the resonance frequency of the flexible suspension, the value of which lies in the frequency range 1.0–6.0 Hz. The combined receiver adjusted with preamplifiers in the frequency range 50–1000 Hz has identical amplitude (mismatching between channels is not more ± 0.1 dB) and phase (channels misalignment is not more $\pm 3°$) characteristics.

The combined receiver within its working frequency range may be considered as a point receiver. Its characteristics are as follows.

(1) A circular directivity diagram for a hydrophone and cosine directivity diagram for each of three channels of the particle velocity receiver show a cosine directivity diagram for each channel of the receiver under multiplicative processing, whereas they yield a cardioid directivity diagram for each channel of the combined receiver while on additive processing.

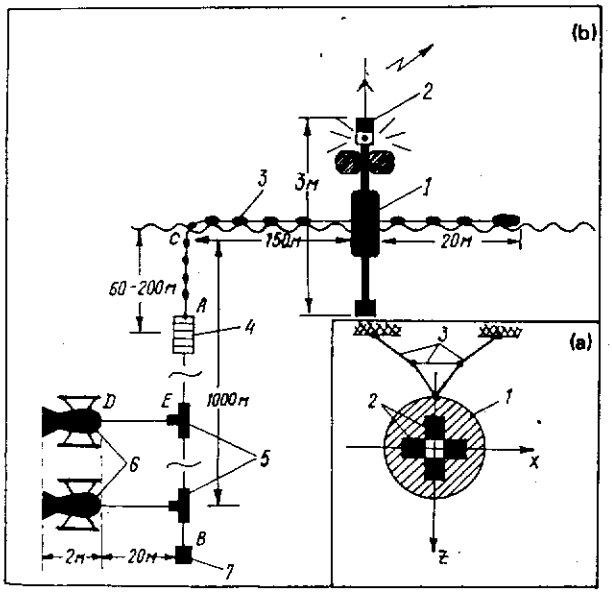

FIG. 1. Deployment scheme for the particle velocity receiver (a) and telemetry combined system (b). The following notation is introduced: (a) 1—single hull, 2—transducers, 3—rubber cords, (b) 1—container with the apparatus and power supply, 2—radio transmitter, 3—horizontal cable line with floats, 4—deep-water buoyancy, 5—cable junction boxes, 6—combined acoustic module, 7—load.

(2) In the working frequency range the directivity diagram of the receiver is frequency-independent.

(3) The combined receiver being a receiver of the energy flux density vector distinguishes right–left or (upper–lower) half-space that allows for the examining of the directionality properties of composite acoustic fields using a point receiver. This is very important for infra- and sound frequency ranges.

3. Telemetry combined system

Investigations of the vector-phase characteristics of underwater ambient noise were carried out using bottom cable systems and telemetry moored or drifting deep-water instruments transmitting information by a radiochannel to the shore or ship. The bottom–system arrangement has been described in Refs. 1 and 14. The general configuration of the combined deep-water eight-channel telemetry system is sketched in Fig. 1. The telemetry system remained operational when wind force was 6. Cancellation of the forced variations and variations naturally arising in the cable line under the effect of the sea surface roughness is performed as follows.

(1) The vertical cable line AB has negative buoyancy of not more than 10–15 kg. This negative buoyancy is compensated for by a long chain AC of small floats (lifting capacity of one float is 0.2 kg).

(2) The entire cable line is placed into a vacuum polyurethane plastic "stocking."

(3) The measuring module (Fig. 2) together with the horizontal cable ED has neutral buoyancy with error ± 0.05 kg. Tilt of the module is not more than $\pm 5°$.

A number of field studies have revealed that the smallest drifting of the measuring system relative to water stretches the cable ED and acoustic module horizontally (Fig. 1). The acoustic array restores its working equilibrium state in 45–60 min after setting the system. The vertical cable line may be connected with the acoustic array at any depth from 20 to 1000 m.

The system remains autonomous for 15 days. The Radiotelemetry is operational to range 15 km.

II. RESULTS OF INVESTIGATIONS

In the general case the acoustic field may be represented by a superposition of three idealized—active, reactive, and diffusive—fields. For the simple case, the active field is a plane traveling wave field in an infinite homogeneous medium. An example of the reactive field is a standing wave, and the diffuse field represents the reactive field that is formed, for example, by statistically independent sources of the reverberation field.

The energy density of the composite acoustic field will be determined by the energy densities sum of each of these addenda. However, only the active component determines this field intensity, since the energy flux density vector of the reactive and diffusive fields is equal to zero.[34,36]

Thus, while calculating the energy density and energy flux density vector of the composite field it is possible to make its classification. The sum of the active and reactive

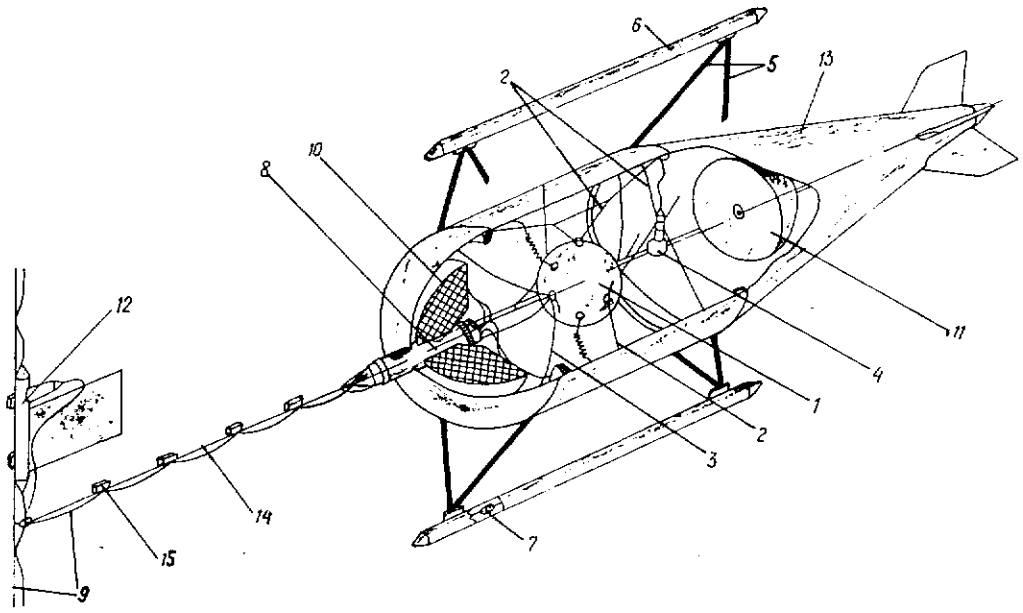

FIG. 2. Combined acoustic module. Notation: 1—three-component particle velocity receiver, 2—flexible rubber cords, 3—movements limiting thread, 4—hydrophone, 5—float's bars, 6—float, 7—tilt adjuster, 8—container, 9—cable, 10,11—buoyancy, 12—cable box, 13—sonar dome cover made of soft material, 14—polypropylene halyard, 15—small floats.

components represents the anisotropic field; a diffusive component represents the isotropic field.

In this part of the paper we present an algorithm of splitting the field into the anisotropic and isotropic components. Their qualitative relationship depends upon the sea surface wind speed, properties of the vertical and horizontal noise power flows, and statistical characteristics of the acoustic pressure and particle velocity in the anisotropic and isotropic fields.

A. Algorithm for splitting the noise field into its anisotropic and isotropic components

The underwater ambient noise field (called the total field in the present work) can be represented as a superposition of statistically independent anisotropic and isotropic fields.[37] In this case the instantaneous values $P(t)$ and $\mathbf{V}(t)$ of the total field will be written as

$$P(t) = P_a(t) + P_i(t),$$

$$\mathbf{V}(t) = \mathbf{V}_a(t) + \mathbf{V}_i(t),$$

where $P_a(t)$, $\mathbf{V}_a(t)$ represents the anisotropic field and $P_i(t)$, $\mathbf{V}_i(t)$ represents the isotropic field.

In the total field resulting from the active, reactive, and diffuse components the coherence function for the random processes $P(t)$ and $V_r(t)$ may take values $0 \leqslant \gamma^2_{PV_r} \leqslant 1$.

In the anisotropic field of a plane traveling in the r wave direction in an homogeneous medium, the random values $P(t)$ and $V_r(t)$ are correlated and $\gamma^2_{PV_r} = 1$. In the isotropic field which is diffusive by its nature $P(t)$ and $V(t)$ are not correlated and, therefore, $\gamma^2_{PV_r}(f) = 0$ (Ref. 36).

Since the energy densities of the total and anisotropic fields are experimentally calculated, the diffuse field energy density will be obtained by subtracting the anisotropic field energy from that of the total field. Splitting of the total field into the anisotropic (coherent) and isotropic (incoherent) components enables us to estimate the contributions of these components to the real noise field and to study properties of each of the components.

In order to divide the total field into the anisotropic and isotropic components, the following algorithm has been developed. Find the power spectra for the anisotropic and isotropic fields. According to a spectrum theorem,[38] the total field power spectrum can be represented as:

$$S_{p^2}(f) = S^a_{p^2}(f) + S^i_{p^2}(f),$$

where $S^a_{p^2}(f)$ is the anisotropic field power spectrum;

$S^i_{p^2}(f)$ is the same for the isotropic field.

Similarly, since $P(t)$ and $V(t)$ are physically equal:

$$S_{V^2}(f) = S^a_{V^2}(f) + S^i_{V^2}(f).$$

For the anisotropic field

$$S^a_{p^2}(f) = |S^a_P|^2, \quad S^a_{V^2}(f) = |S^a_V(f)|^2.$$

Moreover, the reciprocal spectrum modulus is

$$|S_{PV}(f)| = |S^a_P(f)||S^a_V(f)|.$$

Since $P_a(t)$ and $V_a(t)$ are also equal characteristics of the field, hence, owing to a virial theorem,[32] we can write this equation as

$$S^a_{V^2}(f) = m^2(f) S^a_{p^2}(f).$$

Here $m^2(f)$ is determined by signal receiving and processing paths and is dimensionless because $P(t)$, $V(t)$ are measured per units of pressure. So, it is natural to put

$$m^2(f) = S_{V^2}(f)/S_{p^2}(f).$$

Then

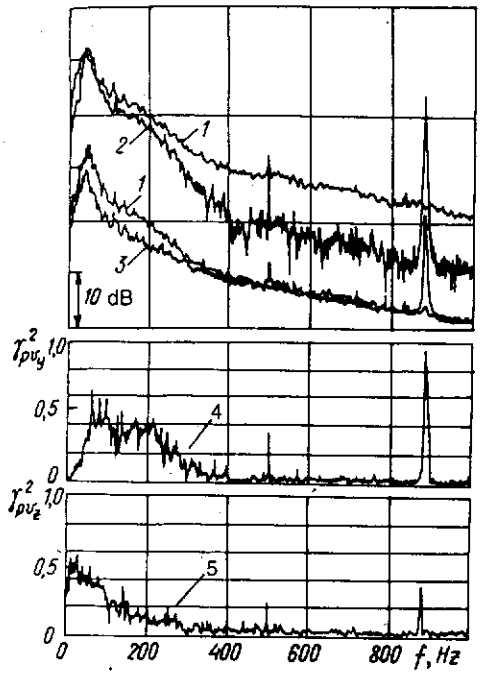

FIG. 3. Spectral densities and noise coherence functions during calm weather. Averaging time is 60 s. The spectrum pairs spacing is 20 dB. 1—total field, 2—anisotropic field, 3—isotropic field, 4—$\gamma^2_{pV_y}(f)$, 5—$\gamma^2_{pV_z}(f)$.

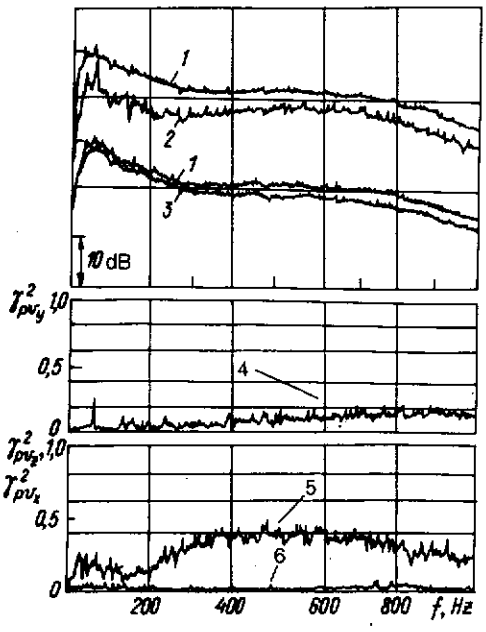

FIG. 4. Spectral densities and noise coherence functions under the steady-state surface roughness. Wind speed is 10 m/s. Averaging time is 60 s. The spectrum pairs spacing is 20 dB. 1—total field, 2—anisotropic field, 3—isotropic field, 4—$\gamma^2_{pV_y}(f)$, 5—$\gamma^2_{pV_z}(f)$, 6—$\gamma^2_{pV_x}(f)$.

$$|S_{PV}(f)| = m(f)|S^a_P(f)|^2 = m(f)S^a_{p^2}(f).$$

Thus we find the spectra:
for the anisotropic component

$$S^a_{p^2}(f) = |S_{PV}(f)|/m(f),$$

for the isotropic

$$S^i_{p^2}(f) = S_{p^2}(f) - S^a_{p^2}(f).$$

B. Ratio of the anisotropic and isotropic components in the noise field

Using the algorithm of total field splitting into the anisotropic (coherent) and isotropic (incoherent) fields, we perform analysis of underwater ambient noise. Now we present the results of noise studies recorded at the same point in coastal waters under calm and stormy weather conditions. The experimental conditions were as follows. The measurement point was 40 km offshore and the water depth was 250 m. A combined receiver was placed at a depth of 230 m. The x axis of the vector receiver was directed along the shore, the y axis directed to the open sea, and the z axis directed vertically. In the maximum directionality diagram of the y axis there was placed a stationary source radiating 500- and 880-Hz tones.

Figure 3 implies the following meteorological conditions: wind speed 1–2 m/s, light sea surface roughness without swell.

In Fig. 4 the conditions are 10 m/s wind speed and developed steady-state sea surface roughness with swell. Direction of the surface roughness and swell is the same as that of the y axis.

In addition to Figs. 3 and 4, digital values of the following characteristics are presented in Tables I and II; (1) coherence functions $\gamma^2_{PV_y}(f)$ and $\gamma^2_{PV_z}(f)$ [for the random processes $P(t)$ and $V_y(t)$, $V_Z(t)$, respectively]; (2) the differences between spectral densities of the total field and corresponding values of the anisotropic ΔN_a(dB) and isotropic ΔN_i(dB) fields; (3) values of the anisotropic field spectral density in percent of the total field, N_a(%).

The calculations were carried out at the 6% band in the continuous part of the spectrum and at the 2-Hz band for 500- and 880-Hz tone signals.

When calm weather conditions take place, underwater ambient noise is seen to be divided into coherent and incoherent parts as follows (Fig. 3, Table I). The coherent component is being observed only at frequencies below 400 Hz. It seems more likely that this coherent component is due to shipping noise and besides, coherence occurs at the horizontal plane along the y axis only. The coherence along the x axis, $\gamma^2_{PV_x}(f)$, is small compared to that along the y and z axes, $\gamma^2_{PV_{y,z}}$, and is not shown in Fig. 3. In the coherent noise region (60–300 Hz) and for the 500- and 880-Hz tone signals, the anisotropic field is 55%–95% of the total field. That there are no tone signals of 500 and 880 Hz in the isotropic field spectrum is an evidence of the efficiency of the algorithm used. It should be noted that though the anisotropic field power is the larger component in the frequency range 60–300 Hz, the anisotropic and isotropic fields powers are of equal order. Above 300 Hz the isotropic component seems to be dominant over the anisotropic one in the total field noise spectrum, the former being one or two orders greater than the latter (see Table I, 400 Hz, 600 Hz).

The anisotropic field spectrum becomes more indented at frequencies above 300 Hz, i.e., in that part of the spec-

TABLE I. Characteristics of noise field at wind speed 1–2 m/s.

f, Hz	60	100	200	300	400	500	600	880	900
γ^2_{pVy}	0.372	0.340	0.382	0.211	0.088	0.442	0.017	0.985	0.060
γ^2_{pVz}	0.415	0.315	0.153	0.045	0.077	0.299	0.017	0.382	0.130
ΔN_a, dB	1.7	1.5	2.6	5.3	11.0	1.7	15.0	0.2	7.5
ΔN_i, dB	4.8	5.3	3.5	1.3	0.6	4.8	0.2	13.0	0.9
N_a, %	68	71	55	29	8	68	3	95	18

trum, in which the isotropic field constitutes most of the total field. The isotropic field spectrum is smoother as compared with that of the anisotropic field throughout the frequency range.

Spectral density of the anisotropic field has greater variance in the higher frequency range than at frequencies below 400 Hz. Under stormy weather conditions (Fig. 4, Table II) the anisotropic component dominates the isotropic throughout the frequency range, however, they are the same order values. The anisotropic field spectrum is greater than the spectrum of the isotropic field. An absolute error in the calculations of the anisotropic and isotropic fields spectral densities does not exceed $\pm$ 10%, i.e., $\pm$ 0.4 dB.

C. Anisotropic and isotropic fields properties

A comparison analysis on spectral characteristics of the total, anisotropic, and isotropic fields performed for various wind speeds (Figs. 3 and 4) reveals the mechanisms of generating the dynamic noise field coherent and incoherent components. When wind is light (Fig. 3, Table I), in the frequency range 60–300 Hz, both the anisotropic and isotropic components are seen. It seems most likely that shipping is one of the main sources of the anisotropic field in this frequency range under calm weather conditions. In fact, according to experimental observations (see, for example, Ref. 39), noise due to distant shipping is dominant in ambient noise over this frequency range.

The horizontal component of the shipping noise, in our case, is in the direction from the open sea to the shore; its vertical component can be directed either toward the sea floor or the surface, depending upon frequency, distance to the source, and depth. The spectra of the total and anisotropic fields show the characteristic of upward bulging in the frequency range 60–300 Hz, whereas the isotropic field spectrum shows downward bulging.

In the frequency range 300–1000 Hz the isotropic component prevailings in the total field. Table III shows the dependence on frequency of the steepness in falloff of the power level spectral density and its anisotropic and isotropic components, by using the data from Figs. 3 and 4. (Data for Fig. 3 are represented by the numerator, those for Fig. 4 by the denominator.)

It follows from Table III that the isotropic field spectrum for the light surface roughness (Fig. 3) varies with frequency as $1/f^2$ in the range 100–1000 Hz; at frequencies above 400 Hz (i.e., above that frequency range where noise of distant shipping occurs) the anisotropic field spectrum decreases as $1/f^3$. As it has been shown by the investigations carried out in various regions in the ocean, when: (1) the distance from shore was more than 10 km, (2) water depths were greater than 100 m, and (3) steady-state sea-surface wind speed was not more than 2.0–2.5 m/s, then in the frequency range 60–1000 Hz the isotropic component spectrum decreases with frequency as $1/f^{2\pm0.2}$; that of the anisotropic falls as $1/f^{3\pm0.3}$ (in the frequency range above the shipping noise). Moreover, at frequences above 300 Hz the magnitude of the anisotropic field, associated with the ambient noise energy transfer over the ocean, can be two orders less than that of the isotropic field, i.e., that portion of energy which represents a diffusive field in the ocean waveguide and is not transported in space. Maximum value of the difference of the spectral density levels of the total and anisotropic fields may reach 18–20 dB.[21–25] As a result, the spectrum of the anisotropic field of dynamic noise is less than the corresponding spectrum of the isotropic field.

On increasing the near-sea surface wind and the surface roughness the dynamic noise spectra tend to be changed (Fig. 4, Table II). Also, frequency-dependent steepness of the falloff in the total, anisotropic and isotropic fields spectral levels changes. Contribution from the anisotropic and isotropic fields to the total field of ambient noise becomes equal throughout the frequency range (Table II). Thus, the

TABLE II. Characteristics of noise field at wind speed 10 m/s.

f, Hz	60	100	200	300	400	500	600	880	900
γ^2_{pVy}	0.034	0.018	0.025	0.025	0.035	0.046	0.091	0.090	0.112
γ^2_{pVz}	0.190	0.192	0.129	0.334	0.415	0.400	0.421	0.387	0.301
ΔN_a, dB	6.7	6.3	8.0	4.9	3.9	4.1	3.3	3.9	3.9
ΔN_i, dB	0.7	0.6	1.1	1.7	2.0	2.1	2.0	2.9	2.7
N_a, %	21	23	16	32	41	39	47	41	41

TABLE III. Steepness of falloff in the noise spectral density level (– dB/oct).

Δf, Hz	Total field	Anisotropic field	Isotropic field
100–200	4.5/3.6	3.2/3.1	6.2/4.0
200–400	10.0/2.6	16.3/ + 0.8	5.8/4.0
300–600	7.7/0.5	13.0/ + 1.3	5.8/1.0
400–800	6.3/2.8	8.7/2.6	6.2/2.5
500–1000	6.8/8.2	8.2/8.7	6.0/8.0

steady-state sea surface roughness generates coherent acoustic noise fields with approximately identical power. The character of the anisotropic field coherence in the horizontal plane differs from that in the vertical plane (see Fig. 4, curves 4,5,6; Table II). Moreover, in the horizontal plane the coherence is observed along the y axis and is negligibly small along the x axis. However, experimental conditions assume that the y-axis direction is similar to the direction of the sea surface roughness and of the water-surface wind propagation (see Sec. II B). In the frequency range 400–600 Hz the coherence in the vertical plane (Fig. 4, curve 5) has distinct maximum.

The experimental studies show that the above discussed coherent properties of underwater ambient dynamic noise may be treated as fundamental. Now we present (in addition to Fig. 4) the results of the deep open ocean ambient noise studies (Figs. 5 and 6).

The experimental conditions were as follows: the water depth was 3600 m; underwater sound channel axis was located at a depth of 1200 m; the sound velocity near the surface was larger than that near the sea floor; wind speed was 12 m/s; there was steady-state sea surface roughness with swell; wind, surface roughness and swell were in the same direction. A telemetry system was placed within a near-field shadow zone, relative to a receiving ship, at a distance of 10–15 km. The receiving ship was drifting while on "silent ship" operation. A combined receiver was located at a depth of 250 m. The x axis of the receiver was in the same direction as the surface roughness propagated.

In Fig. 5 are presented the spectral densities for the total, anisotropic, and isotropic fields. The spectra are calculated using the algorithm for total field splitting (Sec. II A).

Figure 6 shows the coherence function $\gamma^2_{PVx}(f)$, $\gamma^2_{PVy}(f)$, $\gamma^2_{PVz}(f)$ and phase spectra $\varphi_{PVx}(f)$, $\varphi_{PVy}(f)$, $\varphi_{PVz}(f)$ corresponding to Fig. 5. By comparing Fig. 4 with Figs. 5 and 6 one can conclude that the dynamic ambient noise properties in coastal area at a wind speed of 10 m/s are also characteristic of deep open ocean at a wind speed of 12 m/s. The difference is that in the case with deep open ocean the anisotropic coherent field (Fig. 5, curve 2) in the frequency range 300–600 Hz contributes more to the total field than the isotropic diffusive field does (Fig. 5, curve 3).

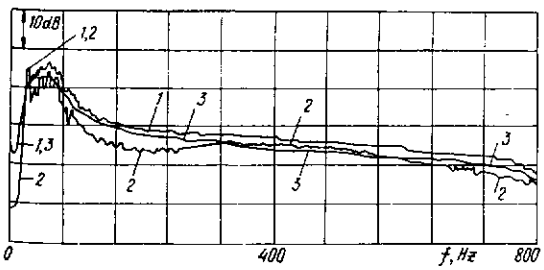

FIG. 5. Spectral densities under the steady-state surface roughness. Wind speed is 12 m/s. Averaging time is 200 s. 1—total field, 2—anisotropic field, 3—isotropic field.

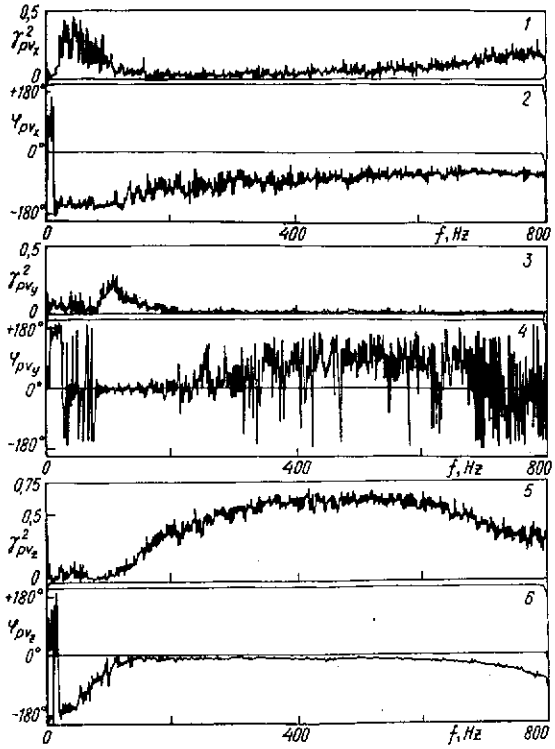

FIG. 6. Coherence functions and the corresponding phase spectra. Averaging time is 200 s.

In the horizontal plane the coherence is observed in the dynamic ambient noise field (200–800 Hz) only along the x axis, i.e., along the direction in which the sea surface roughness propagates (Fig. 6, curve 1). The spectrum $\varphi_{PVx}(f)$ (curve 2) indicates that at frequencies above 200 Hz the noise energy in the horizontal plane arrives there from one direction. In our case this direction is the same as for the surface roughness propagating "forward," that is, the horizontal flow of the noise power transfers the energy in the direction of the sea surface roughness propagation. In the direction perpendicular to the surface roughness direction the coherence function $\gamma^2_{PVy}(f)$ above 200 Hz is negligibly small compared with $\gamma^2_{PVx}(f)$, i.e., in this direction there is no coherence in the noise field (curve 3). The phase difference $\varphi_{PVy}(f)$ is found to be random, that is, the evidence of uncertainity of the power flow direction along the y axis (curve 4). In the vertical plane (Fig. 6, curves 5 and 6) the coherence gains its maximum values in the frequency range 300–600 Hz. The vertical coherent component accounts for about 40% from the total field (Table II) when the wind speed is 10 m/s in this frequency range, and it is almost 60% (Fig. 6, curve 5) in the case in which wind speed reaches 12

m/s. In the frequency range 200–600 Hz the noise energy transfer through the horizontal plane occurs in the surface-bottom direction, which is indicated by the phase spectrum $\varphi_{PV_z}(f)$ (Fig. 6, curve 6).

Thus, the anisotropic field in ambient noise is represented by horizontal and vertical components. Each of the components is expressed by a coherent link between the acoustic pressure and the corresponding component of the particle velocity. Here arises a question—do these components correlate with each other? In Fig. 7 the coherence function and phase spectra between orthogonal components of the particle velocity are shown for the noise field whose spectra are presented in Fig. 4. From Fig. 7 it follows that $\gamma^2_{V_xV_y} = \gamma^2_{V_xV_z} = \gamma^2_{V_yV_z} = 0$, and their phase spectra are seen to be random throughout the frequency range studied. Hence, the orthogonal components of the particle velocity $[V_x(t), V_y(t), V_z(t)]$ are incoherent with each other in the field of dynamic environmental noise. From here it follows that the horizontal and vertical components are believed to be incoherent (uncorrelated).

Thus, a model of dynamic noise in the ocean can be as follows. The acoustic noise field is seen to represent a superposition of the isotropic (incoherent) and anisotropic (coherent) fields, whose energy contribution to the total field is determined by the degree of the sea surface roughness. The isotropic field contributes much to the total field energy and can gain values greater than 90% from the total field under calm weather conditions. The isotropic component represents a diffusive field, whose energy is as if it were "frozen" in the ocean waveguide and is not transported in space. The sea surface roughness is found to be a source of energy pumping to the diffusive field, a portion of the anisotropic field energy being also "pumped" through the mechanisms of the scattering there. The anisotropic field is represented by a superposition of two uncorrelated fields, one of which transports the energy in the vertical plane in the direction of the surface bottom, another-in the horizontal plane in the direction of propagation of the surface roughness.

D. Statistical properties of the anisotropic and isotropic fields

Statistical characteristics of the random values $P(t), \mathrm{V}\{V_x(t), V_y(t), V_z(t)\}$ in the anisotropic and isotropic fields can be estimated in the following approximation.

Let us assume that the anisotropic and isotropic fields are statistically independent;[37] that pressure and particle velocity are statistically independent and Gaussian; that the anisotropic field is expressed as a local plane wave field with a determinate link between the pressure and particle velocity; and that the pressure and the particle velocity in the anisotropic field are Gaussian.[22] Under the assumptions such as shown in Appendix, we have the following ratios of the normalized variances of the total field energy density $D(P^2)$ and energy flux $D(PV)$ for the anisotropic component

$$\eta_a = \frac{D(P^2)}{D(PV)} = 1,$$

for the isotropic component

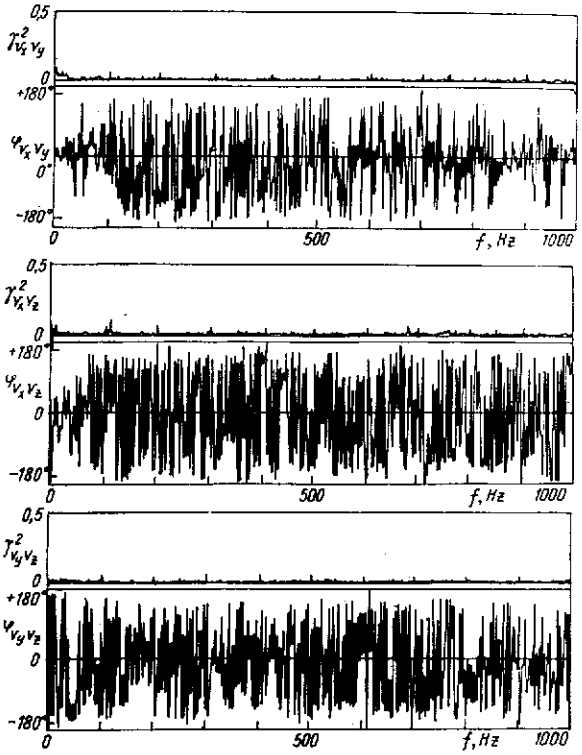

FIG. 7. Coherence functions for the particle velocity orthogonal components and the corresponding phase spectra. Averaging time is 60 s.

$$\eta_i = \frac{D(P^2)}{D(PV)} = 2,$$

and for the total field consisting of the anisotropic and isotropic components

$$1 \leqslant \eta \leqslant 2.$$

Hence, if the above assumptions are true for the field of underwater ambient noise, then depending upon the ratio of the anisotropic and isotropic components in this field η will take on values $1 \leqslant \eta \leqslant 2$.

Figure 8 shows the coherence function of a signal from a local source against ambient noise. The experimental conditions are similar to those associated with Fig. 3. The local source is in the x direction. Since the experiment was carried out during calm conditions, the isotropic component must be dominant in the total field of the dynamic noise (see Secs. II B and II C), except those frequencies at which radiation from the local sources is observed. Thus, by virtue of the coherence function spectrum one can determine frequency intervals in which the noise field is considered to be isotropic or anisotropic with high reliability.

In Fig. 8 it follows that in the frequency ranges 50–300 Hz and 500–550 Hz noise is dominated by radiation from the local source. The coherence function for frequencies at which the radiation occurs is 0.5–0.95, therefore, the field in these frequency ranges is anisotropic (except several frequencies within the ranges considered, where there is no radiation). At bands 300–500 Hz and above 550 Hz the field has prevailing isotropic component that is indicated by the coherence function (Fig. 8). In these frequency ranges one can find such parts of the spectrum where coherence func-

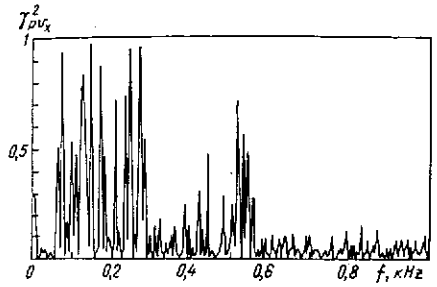

FIG. 8. Coherence function for the acoustic pressure and the particle velocity x component. The x axis is directed to a radiation source. Averaging time is 60 s.

tions values are not higher than 0.1. Let us show the values of η calculated at the 6% band for eight frequencies in Fig. 8 (Table IV).

As it is seen, the variances ratio (within a computational error $\Delta\eta = \pm 0.2$) is near 2 (340,700,800,900 Hz) in the isotropic field; in the anisotropic field it is in the vicinity of unity (150, 250, 520 Hz). In the frequency 420 Hz, where value of the coherence is 0.3, $\eta = 1.5$.

Digital processing of considerable amount of the experimental data on ambient noise has revealed that η values tend to unity in that frequency range where the signal and coherence function are observed to be 0.5 and more (i.e., the anisotropic field is dominant in the total field); if the coherence function is less than 0.3, the value tends to 2; that is the isotropic component makes the main contribution to the total field.

Thus, one can conclude that in the underwater ambient acoustic noise the pressure and particle velocity are Gaussian and, moreover, statistically independent in the isotropic field.

III. CONCLUDING REMARKS

It has been shown in the present paper that description of underwater ambient noise may be limited to the cross-correlation analysis between the pressure and particle velocity of the acoustic field. The studies of the coherence functions of the acoustic pressure and particle velocity components in ambient noise field allow us to: (1) reveal a fundamental phenomenon, that is, transfer of the dynamic ambient noise energy in the direction of the sea surface roughness propagation; (2) to state the relationship between the anisotropic and isotropic components in the dynamic noise field; and (3) to evaluate statistical characteristics of the acoustic pressure and particle velocity of ambient noise.

It seems hard to overestimate the efficiency of the present technique in physical acoustics of the ocean and aeroacoustics. Here, of primary importance are investigations of the phenomenon such as compensation of counterflows of the energy[28] and its utilization in studies on a fine spectral structure of ambient noise both in hydro-and aeroacoustics. Also, it seems interesting to study properties of the diffusive field for estimating power of the reverberation sources in the ocean as well as for examining the mechanism of sound generation while breaking individual wind surface waves.

These investigations appear to be perspective and vital, so technical difficulties associated with measurements of the particle velocity components should be overcome.

TABLE IV. Degree of the noise field isotropy.

f, Hz	150	250	340	420	520	700	800	900
η	1.0	1.2	1.9	1.5	1.1	2.0	2.2	2.1

ACKNOWLEDGMENTS

The author would like to express gratitude to Academician V. I. Ilyichev and Professor David Farmer (Institute of Ocean Sciences, Canada) for fruitful discussions and advice. He is also indebted to V. Dzyuba, Yu. Khvorostov, V. Kuleshov, A. Fedoseenkov, and P. Salnikov for assisting and to L. Lee for translating.

APPENDIX

We find a ratio of normalized variances of the energy density $D(P^2)$ and energy flow density $D(PV)$, assuming that the random values $P(t)$ and $V(t)$ correspond to terms in Sec. II D.

In the anisotropic field there exists a linear relation between pressure and particle velocity modulus $P(t) = bV(t)$, where b is impedance of a medium.

The acoustic energy density E is defined by the expression $E = P^2$ and the acoustic energy flow density by $|\mathbf{I}| = |P\mathbf{V}|$. Let $P(t)$ and $\mathbf{V}(t)$ be scalar-and vector-centered Gaussian random processes, respectively. Powers of the processes are made to be nondimensional by the corresponding normalization: $D(P) = D(V) = 1$, where V is the particle velocity projection in the wave propagation direction. For the anisotropic component, owing to the relation $P(t) = bV(t)$, we proceed from the random value P to the value of the energy flow density vector projection on the energy propagation direction $I(t) = P(t)V(t) = P^2(t)/b$ and then transform the density function of the distribution $\alpha(P)$ of the acoustic pressure values $P(t)$ to those for $\alpha(I)$ of the values $I(t)$. Therefore, we obtain

$$\alpha(I) = \frac{b^{1/2}}{\sqrt{2\pi}\sigma_p} \times \frac{\exp(-Ib/2\sigma_p^2)}{\sqrt{I}}. \tag{A1}$$

The values I are taken as positive and $\sigma_p^2 = D(P)$.

By Eq. (A1) it is easy to derive the flow density variance:

$$\begin{aligned} D(PV) &= D(I), \\ D(PV) &= \langle I^2 \rangle - \langle I \rangle^2 \\ &= 2\sigma_p^2/b = 2D(P)D(V)/b^2 = 2/b^2. \end{aligned} \tag{A2}$$

In order to find the energy density variance, it is reasonable to consider, due to the above determination for E, that in Eq. (A2) $b = 1$. Thus, $D(P^2) = 2D(P)D(V) = 2$.

Due to that the processes $P(t)$ and $V(t)$ are considered as independent. In the isotropic field the energy flux density variance is $D(PV) = D(P)D(V) = 1$.

Therefore, we obtain the following ratios of the normal-

ized variances for the anisotropic field:

$$\eta_a = D(P^2)/D(PV) = 2D(P)D(V)/2D(P)D(V) = 1,$$

and for the isotropic field,

$$\eta_i = D(P^2)/D(PV) = 2D(P)D(V)/D(P)D(V) = 2.$$

For the total field, the processes $P(t)$ and $V(t)$ are defined by the expressions

$$P(t) = P_a(t) + P_i(t), \quad V(t) = V_a(t) + V_i(t).$$

Here the indices a and i are the anisotropic and isotropic components, respectively. Moreover, accounting for these components independence as well as their fields centering, we obtain

$$\begin{aligned}\langle (PV)^2\rangle &= \langle [(P_a + P_i)(V_a + V_i)]^2\rangle \\ &= \langle (P_a V_a)^2\rangle + \langle P_a^2\rangle\langle V_i^2\rangle + \langle P_i^2\rangle\langle V_a^2\rangle \\ &\quad + \langle (P_i V_i)^2\rangle, \quad \langle PV\rangle = \langle P_a V_a\rangle.\end{aligned}$$

The flow density variance is

$$\begin{aligned}D(PV) &= \langle (PV)^2\rangle - \langle PV^2\rangle \\ &= \langle (P_a V_a)^2\rangle - \langle P_a V_a\rangle^2 + \langle (P_i V_i)^2\rangle - \langle P_i V_i\rangle^2 \\ &\quad + \langle P_a\rangle^2\langle V_i\rangle^2 + \langle P_i\rangle^2\langle V_a\rangle^2 \\ &= D(I_a) + D(I_i) + D(P_i)D(V_a) + D(P_a)D(V_i).\end{aligned}$$

In accordance with that, the energy density variance is

$$\begin{aligned}D(P^2) &= \langle P^4\rangle - \langle P^2\rangle^2 \\ &= \langle (P_a + P_i)^4\rangle - \langle (P_a + P_i)^2\rangle^2 \\ &= \langle P_a^4\rangle + \langle P_i^4\rangle + 6\langle P_a^2\rangle\langle P_i^2\rangle - \langle P_a^2\rangle^2 \\ &\quad - 2\langle P_a^2\rangle\langle P_i^2\rangle - \langle P_i^2\rangle^2 \\ &= D(P_a^2) + D(P_i^2) + 4D(P_a)D(P_i).\end{aligned}$$

Powers of the $P(t)$ and $V(t)$ are identical and this implies

$$D(P_a) = D(V_a), \quad D(P_i) = D(V_i).$$

Since $P_a(t)$ and $V_a(t)$ and $P_i(t)$ and $V_i(t)$ are Gaussian, then

$$D(P_a^2) = 2D^2(P_a), \quad D(P_i^2) = 2D^2(P_i),$$
$$D(I_a) = 2D(P_a)D(V_a), \quad D(I_i) = D(P_i)D(V_i).$$

Substituting these expressions into the equation for the variance ratio:

$$\eta = \frac{D(P^2)}{D(PV)} = \frac{D(P_a^2) + D(P_i^2) + 4D(P_a)D(P_i)}{D(I_a) + D(I_i) + D(P_i)D(V_a) + D(P_a)D(V_i)}$$

yields the following for η:

$$\eta = \frac{2[D(P_a) + D(P_i)]^2}{[D(P_a) + D(P_i)]^2 + D(P_a^2)}.$$

Taking into consideration that $D(P_a) + D(P_i) = D(P)$ is the total fields invariance, we obtain the equation that is convenient for analysis:

$$\eta = \frac{2D^2(P)}{D^2(P) + D^2(P_a)},$$

from which it follows that depending on the degree of total field isotropy, η will take the values $1 \leqslant \eta \leqslant 2$.

[1] L. N. Zakharov, S. A. Ilyin, V. I. Ilyichev, and V. A. Shchurov, "Vector-phase methods in ocean acoustics," in *Problemy akustiki okeana*, edited by L. M. Brekhovskikh and I. B. Andreyevoi (Nauka, Moscow, 1984), pp. 192–204 (in Russian).

[2] L. N. Zakharov, "Methods of calibrating hydroacoustic receivers of the particle velocity of medium," Akust. Zh. **17** (4), 558–562 (1971) (in Russian).

[3] L. N. Zakharov and S. N. Rzhevkin, "Vector-phase measurements in acoustic fields," Akust. Zh. **20** (3), 393–401 (1974) (in Russian).

[4] T. Kendall, U.S. Patent No. 2,582,992 (1943) (1952).

[5] T. Kendall, U.S. Patent No. 2,597,005 (1943) (1952).

[6] C. Leslie, T. Kendall, and T. Jones, "Hydrophone for measuring particle velocity," J. Acoust. Soc. Am. **28**, 711–715 (1956).

[7] L. M. Lewandowski, U.S. Patent No. 4,173,748 (1978) (1979).

[8] W. P. Mason, U.S. Patent No. 2,838,741 (1953) (1958).

[9] G. Rasmusser, "Practical application of intensity measurement," in Internoise 84, New York, 1984, Vol. 2, pp. 1133–1138.

[10] H. Robert, U.S. Patent No. 3,603,921 (1968) (1971).

[11] Technical Review, Sound intensity, Bruel&Kjaer, No. 3, 1982.

[12] J. Tichy, "Basic intensity flow relationships in acoustic fields," in Internoise 84, New York, 1984, Vol. 2, pp. 1149–1154.

[13] S. N. Rzhevkin, "On the variations of bodies placed into fluid under the action of sound wave," Vestnik of Moscow University, No. 1, 52–61 (1971) (in Russian).

[14] Ye. L. Gordienko, L. N. Zakharov, S. A. Ilyin, V. I. Ilyichev, A. A. Slutskov, F. A. Toporovsky, Yu. V. Penkin, and V. A. Shchurov, "Facility for measuring the noise sources parameters," A. s. 953468 USSR, 1981 (in Russian).

[15] T. Y. Chung, "Fundamental aspects of cross-spectral method of measuring acoustic intensity," CETIM, Senlis, France, 1981, pp. 1–10.

[16] F. T. Fahy and S. T. Elliott "Practical considerations in the choise of the transducers and signal processing techniques for sound intensity measurements," CETIM, Senlis (France), 1981, pp. 33–34.

[17] H. Kutter, "An analogue intensity meter based on the gradient principle," CETIM, Senlis (France), 1981, pp. 61–67.

[18] P. G. Mathur, "A stochastic analysis for cross-spectral density method of measuring acoustic intensity," J. Acoust. Soc. Am. **74**, 1752–1756 (1983).

[19] Technical Review, Sound intensity, Bruel & Kjaer, No. 4, 1982.

[20] J. K. Thompson and T. Kuynk, "Intensity measurement errors in a reactive environment," in Ref. 12, pp. 1143–1148.

[21] Ye. L. Gordienko, L. N. Zakharov, S. A. Ilyin, V. I. Ilyichev, V. A. Shchurov, "Study of the ocean noise field anisotropy," Akusticheskie sredstva i metody osvoyeniya okeana. Vladivostok: DVGU, 1981, pp. 122–126 (in Russian).

[22] V. P. Dzyuba, V. I. Ilyichev, and V. A. Shchurov, "Statistical properties of the acoustic noise field," Tez. dokl. 14-i Vsesoyuz. shkoly-seminara po statisticheskoi gidroakustike (SG-14). Nauka, Moscow, 1986, pp. 32–36 (in Russian).

[23] V. P. Dzyuba, V. I. Ilyichev, and V. A. Shchurov, "Statistical properties of the acoustic noise field in the ocean," Dokl. Akad. Nauk **291** (4), 982–984 (1986) (in Russian).

[24] L. N. Zakharov, S. A. Ilyin, V. I. Ilyichev, Ye. S. Tkachenko, V. A. Shchurov, "Characteristics of the noise field acoustic power flow in coastal area," in Materially 10-i Vsesoyuz. Akust. Konf, Nauka, Moscow, 1983, pp. 56–58 (in Russian).

[25] L. N. Zakharov, S. A. Ilyin, V. I. Ilyichev, Ye. S. Tkachenko, and V. A. Shchurov, "Properties of the noise field power flow in coastal zone," Tez. dokl. 5-go seminara "Acoustic statistical models of the ocean," Nauka, Moscow, 1985, pp. 76–79 (in Russian).

[26] V. A. Shchurov, V. P. Dzyuba, and V. P. Kuleshov, "Investigation of the acoustic noise field in the ocean using the vector-phase techniques," in *Utilization of the Vector-Phase Technique in Ocean Acoustics*, edited by V. A. Shchurova (DVO AN SSSR, Vladivostok, 1989), pp. 5–47 (in Russian).

[27] V. I. Ilyichev, V. A. Shchurov, V. P. Dzyuba, and V. P. Kuleshov, "Investigation of the acoustic noise field in the ocean using vector-phase methods," *Akustika Okeanskoy Sredy*, edited by L. M. Brekhovskikh and I. B. Andreyevoi (Nauka, Moscow, 1989), pp. 144–152 (in Russian).

[28] V. I. Ilyichev, V. A. Shchurov, V. P. Kuleshov, M. V. Kuyanova, "Inter-

action between the acoustic energy flows of ambient noise and local sources in the ocean waveguide," Preprint Tikhookeansky Okeanologichesky Institut DVO AN SSSR, Vladivostok, 1990 (in Russian).
[29] I. S. Bendat and A. G. Piersol, *Random Data: Analysis and Measurement Procedures* (Wiley–Interscience, New York, 1971).
[30] J. W. Horton, *Fundamentals of Sonar* (USNI, Annapolis, MD, 1961).
[31] N. A. Umov, *Equation for Energy Movements into Bodies* (Tip. Ulrich and Shultse, Odessa, 1874) (in Russian).
[32] L. D. Landau and E. M. Lifshitz, *Hydrodynamics* (Nauka, Moscow, 1986) (in Russian).
[33] L. N. Zakharov, "Vector-phase measurements in acoustics," in 7th Vsesoyuz. konf. po inform. akustike. Nauka, Moscow, 1982, pp. 31–50 (in Russian).
[34] S. N. Rzhevkin, *Lectures on Theory of Sound* (Izd. MGU, Moscow, 1960) (in Russian).
[35] G. V. Chechin and O. V. Kobzar "Evaluation of an error due to acoustic scattering on the pressure gradient receiver's hull while calibrating in the near-field of radiator," in *Primeneniye vektorno-fazovogo metoda v akustike okeana*, edited by V. A. Shchurova (DVO AN SSSR, Vladivostok, 1989), pp. 131–136 (in Russian).
[36] S. M. Rytov, Yu. A. Kravtsov, and V. N. Tatarsky, *Introduction to Statistical Radiophysics* (Nauka, Moscow, 1978) (in Russian).
[37] F. Cron and Ch. Sherman "Spatial correlation functions for various noise models," J. Acoust. Soc. Am. **34**, 1732–1736 (1962).
[38] A. A. Kharkevich, *Spectra and Analysis* (GITTL, Moscow, 1957) (in Russian).
[39] G. Wenz, "Acoustic ambient noise in the ocean: Spectra and sources," J. Acoust. Soc. Am. **34**, 1936–1956 (1962).